ORIGINAL PAPER

Chemical structures of odorants that suppress ion channels in the olfactory receptor cell

Yukako Kishino · Hiroyuki Kato ·
Takashi Kurahashi · Hiroko Takeuchi

Abstract It has been proposed that odorant suppression of the cyclic nucleotide-gated (CNG) channel is responsible for olfactory masking. In this study, the effect of odorant chain length and functional group on this suppression was investigated. Because similar suppression has been observed for voltage-gated channels also, we used voltage-gated Na channels in the olfactory receptor cell as a tool for substance screening. These features were then reexamined using CNG channels. Interestingly, both CNG and Na channels were suppressed in a similar manner—carboxylic acids had little effect and suppression became stronger when the chain length of the alcohol or ester was increased. Degree of suppression was correlated with the distribution coefficients (Log D), irrespective of the molecules used. Results obtained here may provide information for the development of novel masking agents based on molecular architecture.

Keywords Olfactory masking · Voltage-gated Na channel · CNG channel · Current suppression · Distribution coefficient

Y. Kishino · T. Kurahashi · H. Takeuchi (✉)
Graduate School of Frontier Bioscience, Osaka University,
Osaka 560-8531, Japan
e-mail: hiroko@bpe.es.osaka-u.ac.jp

H. Kato
Departments of Chemistry and Materials Science,
Graduate School of Science, Osaka City University,
Osaka 558-8585, Japan

Introduction

In human history, olfaction has been continuously important in increasing the quality of life. Odorant molecules have been used not only to induce pleasant senses, but also to suppress unpleasant smells. Such suppressive phenomena in olfaction have been used for long period of time, and are termed olfactory masking. Recently, it has been proposed that olfactory masking is, at least in part, regulated by direct blockage of olfactory transduction channels (cyclic nucleotide-gated (CNG) channels) at the ciliary membrane [1–3]. The suppression ratio in CNG channels for a variety of odorants correlates positively with that observed in human olfactory masking. Furthermore, it has been shown that odorant molecules absorbed from the air have the ability to suppress CNG channels beyond the air/water boundary, indicating that such suppression occurs in the human nose. There are possibilities that olfactory masking can be investigated in further detail by examining the effects of a variety of odorants on CNG channels. However, use of CNG channels for compound screening is accompanied by large difficulties; they are strongly localized to fine (sub-micron diameter) cilia and are gated by cytoplasmic cAMP. Caged compounds could be used to measure the transduction current suppression directly. However, olfactory receptor cells (ORCs) are damaged by strong UV irradiation and by introduction of caged compounds to the cell, and, therefore, the lifetime of cells in such experiments becomes shorter than in conventional patch-clamp experiments.

Interestingly, in parallel, such blockages by odorants are observed also for several types of voltage-gated ion channels that are unrelated to olfactory signal transduction (K channels: [4]; Na and Ca channels: [5]). Although comparison with CNG channel suppression has been performed for a rather limited number of substances, the odorants that

suppress voltage-gated channels overlap with odorants effective on CNG channels. It is possible that the mechanisms causing odorant blockage of voltage-gated channels share the same step(s) as those for CNG channels.

This study was undertaken to investigate the functional structure of odorants that suppress ion channels. At the beginning of the work, we used voltage-gated Na channels in the ORC as a tool for rapid screening. Compared with CNG channels, they have several technical benefits for electrophysiology—they are activated by voltage steps only, show little rundown, and show rapid kinetics that allow one to obtain large numbers of data during recordings. The highlighted features were then re-examined with CNG channels. As for the structure of the odorant molecules, we systematically changed the length of the hydrocarbon chain and the functional group (alcohols, esters, and carboxylic acids). We showed that suppression by alcohols and esters became stronger when the chain length was increased from 4 to 6 and then to 8, and there was a positive correlation between the suppression and the oil/water distribution coefficient (D). Furthermore, among chemicals with carbon chains of similar length but different functional groups, suppression by carboxylic acids was weakest. It is notable that carboxylic acids are almost 100% ionized, dissolve stably in water, and have very small Log D values. The molecular features of these chemicals represent those inducing olfactory masking, and results obtained here will provide information for the development of novel masking agents on the basis of molecular architecture.

Materials and methods

Preparation

ORCs were dissociated enzymatically from the olfactory epithelium of the newt (*Cynops pyrrhogaster*). The experiments were performed under the latest ethical guidelines for animal experimentation at Osaka University, based on international experimental regulations. The dissociation procedures have been described previously [6]. Briefly, before decapitation, the animal was kept at 4°C in a refrigerator for 30 min. The mucosae excised from the nasal cavity were cut into 8 pieces in standard Ringer's solution (for composition, see below). After incubation of the epithelia for 5 min at 35°C in Ringer's solution containing 0.1% collagenase with 0 Ca^{2+} and 0 Mg^{2+} (see below), the tissue was gently rinsed three times with normal Ringer's solution. Finally, the epithelia were mechanically triturated. Isolated cells were plated on concanavalin A-coated glass-bottom dishes (glass thickness 0.08–0.12 mm; Matsunami Glass). Cells were maintained at 4°C, before use within the next

2 days. Throughout the experiments, we selected ORCs lacking cilia to eliminate the possibility of generating responses induced by odorant stimulation.

Recording procedures

Membrane currents were obtained with the whole-cell recording configuration [7]. Patch pipettes were made of borosilicate tubing with a filament (outer diameter 1.2 mm; World Precision Instruments) by using a two-stage vertical patch electrode puller (PP-830; Narishige Scientific Instruments). The pipette resistance was 10–20 MΩ.

In the Na current suppression experiments, the liquid junction potential at the pipette tip was 3.9 mV, and this was subtracted from the data. An inverted microscope (IX70; Olympus) equipped with phase-contrast optics was used for observing and identifying ORCs. The recording electrode was connected to a patch clamp amplifier (Axopatch1D; Molecular Devices). Data were sampled with pClamp version 9.0 (Molecular Devices) at 10 kHz (16 bit, Digidata1322A; Molecular Devices) after low-pass filtration at 1 kHz (4-pole Bessel). The current data were analyzed by an offline computer (Endeavor MT7800; Epson) with Microcal Origin 7.5 software (OriginLab). We defined the peak amplitude of the voltage-gated Na current during the odorant stimuli to be the same timing of peak current obtained in control solution, especially when the inward component was abolished by the drug. Data that showed 90% recovery were used for analyses (Figs. 4, 5, 6). For leak subtraction, in the experiments on the Na channel we used either P/4 leak subtraction or subtraction of the leak current that was obtained in the choline-substituted solution, depending on the purpose of each experiment. In general, P/4 leak subtraction is convenient, but requires much time for recordings, and, in addition, does not provide precise values when the membrane expresses a nonlinear current and voltage (I–V) relationship. Leakage subtraction with choline-substitution requires solution exchanges. But the recording of this procedure is much faster than P/4 subtraction, especially with a fast solution-exchange system. Essentially the I–V curve, activation curve, and inactivation curve were obtained with P/4 subtraction. Suppression ratios were measured with choline-substitution. The background noises and the current fluctuations arising from the channel gatings were reduced by data averaging (30 or 100 waveforms). Pulse to pulse interval was fixed at 300 ms to avoid inactivation. In noise analyses, data that met the criterion correlation coefficient (R^2) > 0.8 from the least-squares fitting and χ^2 < 3.8 from the chi-squared test in the variance–mean plot were used.

In the experiments on CNG channel suppression, the recording pipette was connected to a patch clamp amplifier (Axopatch 200B; Molecular Devices). The signal was

low-pass filtered at 2 kHz and digitized by an A/D converter (sampling frequency 5 kHz) connected to an MS-DOS computer (PC9821, 80486CPU; NEC) or an MS Windows computer (xw8600 workstation; HP) with pClamp 10. Simultaneously, signals were monitored on an oscilloscope and recorded on a chart recorder. Light and odor stimuli, and data acquisition, were regulated by the same computer, by use of original software. The results were analyzed by use of an online workstation computer and plotted by using Microcal Origin 7.5 software. For curve drawings, data were smoothened by 25 Hz low-pass filtration. For odorant stimuli, chemicals were dissolved in perfusion solution (for composition see the section "Solutions"), and this stimulus solution was puff-applied to the cell from a small glass pipette having a tip diameter of 1 μm and was applied by use of a pressure ejection system [8]. The timing of the pressure pulse and the light stimulation are shown above the current traces in the figures as the downward deflection of the traces. Before the experiments on cAMP-induced current, we checked the presence of odor-induced current response. In this study, we selected the ORC having more than five cilia which did not respond to odorant stimulation. Experiments were performed at room temperature (24–25°C). Error bars in all figures indicate SD.

Photolysis of caged compounds

For experiments on the suppression of CNG channels, the ORC was loaded with caged cAMP (adenosine $3'5$-cyclic monophosphate, P1-(2-nitrophenyl) ethyl ester, EMD). Caged cAMP was initially dissolved in DMSO at 100 mM and stored frozen at −20°C in complete darkness. The stock solution was diluted with pipette solution to a final concentration of 1 mM before each experiment. UV light was applied to cover the ciliary region of the solitary cell through an epifluorescent system. Light stimuli were applied with >20 s intervals to avoid adaptation of the cell. A 100-W xenon arc was used to induce photolysis. The timing and duration of light illumination were controlled by a magnetic shutter, and the light intensity was specified by a wedge filter under computer control. The light source was mechanically isolated from the inverted microscope to avoid the transmission of vibrations [9]. Throughout the experiments, we paid particular attention to avoiding current saturation. Especially for measurements of odorant suppression, we fixed the light intensity to induce responses 80–90% of the saturating level, mostly because of the [cAMP]$_i$-dependence of the suppression ratio [3].

Solutions

Normal Ringer's solution contained (mM): 110 NaCl, 4 KCl, 3 CaCl$_2$, 1 MgCl$_2$, 10 glucose, 1 pyruvate, 2 HEPES, 0.001% phenol red, pH 7.2–7.4 adjusted with NaOH for the whole-cell configuration. For isolation of the voltage-gated Na current, after establishment of the whole-cell recording configuration, perfusion solution was switched to (mM): 110 NaCl, 3 CoCl$_2$, 10 HEPES, 35 TEA, pH 7.2–7.4 adjusted with NaOH (TEA [4, 10], Co [11]) that was essentially designed to suppress currents through K channels and Ca channels. Choline solution was used for eliminating voltage-gated Na current (mM): 110 choline Cl, 3 CoCl$_2$, 10 HEPES, 35 TEA, pH 7.2–7.4 adjusted with CsOH. Pipette solution contained (mM): 119 CsCl, 1 CaCl$_2$, 5 EGTA, 10 HEPES, 0.001% phenol red (pH was adjusted to 7.2–7.4 with CsOH) to suppress K channels [12]. Collagenase, concanavalin A, EGTA, and phenol red were purchased from Sigma, KCl from Katayama Chemical, and glucose from Wako Pure Chemical Industries. Other reagents were purchased from Nacalai Tesque.

In the experiments on the CNG channel, Ca-free media were used to abolish the Ca-activated Cl channel (Cl(Ca)). Perfusion solution contained (mM) 110 NaCl, 3.7 KCl, 4 MgCl$_2$, 10 HEPES (pH 7.2–7.4 adjusted with NaOH) and pipette solution (mM) 119 CsCl, 1 CaCl$_2$, 5 EGTA, 10 HEPES, 1 caged cAMP, 0.001% phenol red (pH 7.2–7.4 adjusted with CsOH) were used.

As odorants, chemicals (alcohols: *n*-butanol (C4), *n*-hexanol (C6), *n*-octanol (C8); esters: ethyl acetate (C4), *n*-butyl acetate (C6), *n*-hexyl acetate (C8); and *n*-carboxylic acids: *n*-butyric acid (C4), *n*-hexanoic acid (C6), *n*-octanoic acid (C8)) were purchased from Tokyo Chemical Industry, and C4-ester from Wako Pure Chemical Industries. After mixing of all odorant solutions with perfusion solution and vortex mixing for approximately 30 s, pH was adjusted to 7.2–7.4 with NaOH. In this work, we paid attention to the Na concentration in solutions to observe voltage-gated Na current. Difference in NaOH concentration by pH adjustment was standardized by compensating NaCl concentration in the perfusion solution.

Throughout experiments on suppression of voltage-gated Na current, odorants were applied with the U-tube system [13–15]. Advantages of using this system were:

1 rapid superfusion; and
2 complete solution exchange surrounding the cell, in comparison with a local and partial change by puffer pipette (see Ref. [3]).

The reservoir of the solution was held approximately 25 cm above the recording chamber, and the solution fell into the recording chamber through the tubing by gravity. The tip diameter of the nozzle was approximately 100 μm and the tip of the nozzle was situated approximately 100 μm from the cell. To avoid changes in the capacitance of the recording pipette, the total amount of solution in the dish was kept constant by use of a microtube pump (MP-3N; Tokyo Rika Kikai). In experiments on suppression of cAMP-induced current, puffer application was used for odorant stimulation.

Quantification of the solubility of odorants by gas chromatography

Odorant concentration in the perfusion solution was determined by gas chromatography (6890GC; Agilent Technologies). After odorants were dissolved in the perfusion solution and the pH of the solution was adjusted. The solution was filtered through a syringe-type filter (pore size 0.45 μm) to remove insoluble odorants. Such filtration treatment gave the same result as those obtained by centrifugation or filtration with pore size 0.2 μm.

Samples were injected into the injection port (250°C) which was connected to a DB-5 fused silica column (0.53 mm × 30 m, film thickness 1.0 μm). The column temperature was increased depending on the substance investigated; for example, the initial column temperature was

40°C for C4 alcohol and ester, 60°C for C6 alcohol and ester, 100°C for C8 alcohol and ester and C4–C6 carboxylic acids, and 150°C for C8 carboxylic acid. Thus the initial oven temperature was 40°C (hold 5 min)–150°C (hold 5 min), increasing at 10°C/min to a final temperature of 250°C. The helium pressure was 60 kPa. The flame-ionization detector (FID) temperature was 250°C. The chromatogram corresponding to the FID response is shown in Fig. 1.

Results

Stability and water solubility of odorant molecules

In this study we applied 9 species of odorant molecules (3 × 3; 3 lengths for carbon chains and 3 different
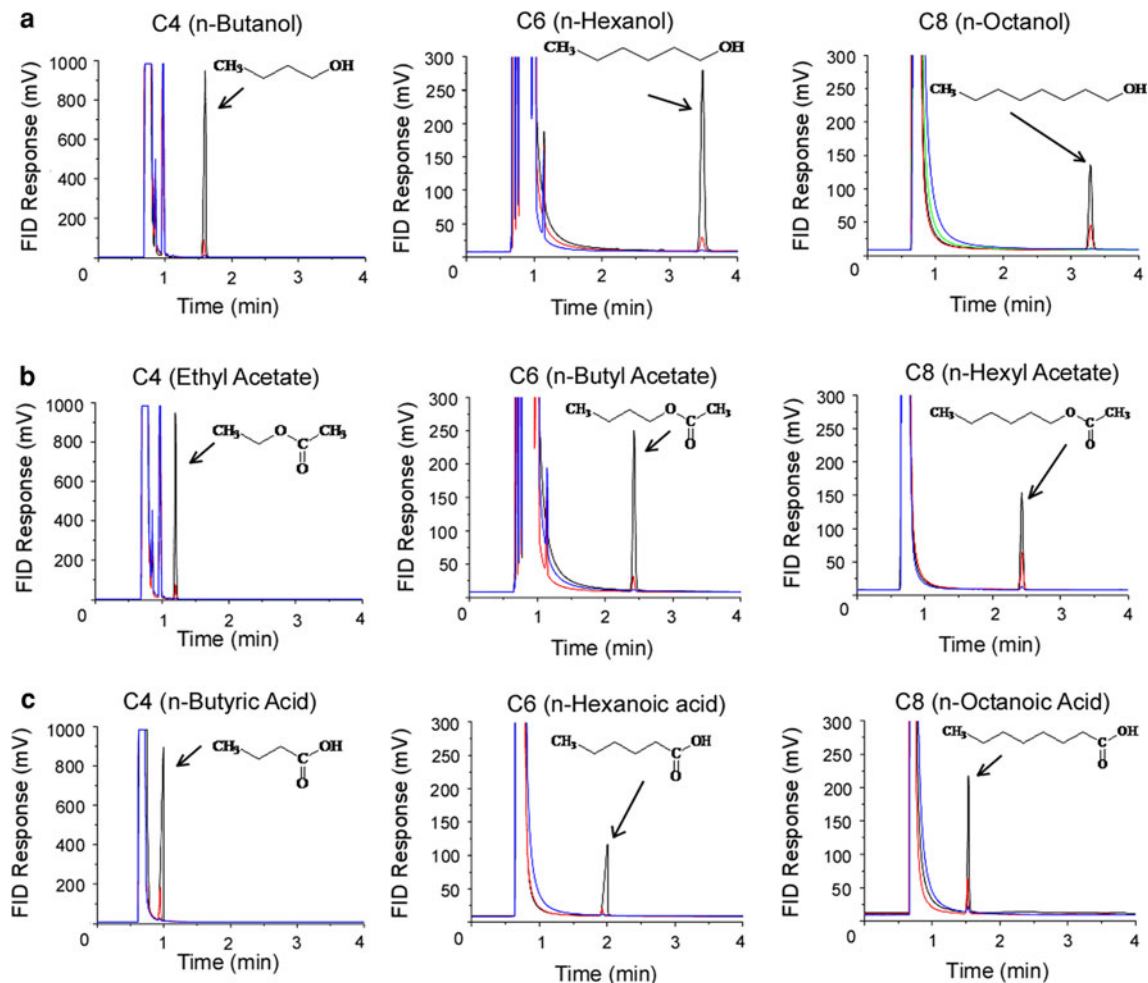
Fig. 1 Gas chromatography assay of odorants in the control solution. Detection voltages were plotted against retention time. The chemical structures of the odorants used are indicated in the figures. *Arrows* indicate the peak of dissolved molecules. **a** Alcohol. C4; 10 mM (*black*), 1 mM (*red*), 0.1 mM (*blue*). C6; 10 mM (*black*), 1 mM (*red*), 0.1 mM (*black*). C8; 2.7 mM (*black*), 0.9 mM (*red*),

0.07 mM (*blue*), 0.007 mM (*green*). **b** Ester. C4; 10 mM (*black*), 1 mM (*red*), 0.1 mM (*blue*). C6; 10 mM (*black*), 1 mM (*red*), 0.1 mM (*blue*). C8; 2.1 mM (*black*), 0.8 mM (*red*), 0.08 mM (*blue*). **c** Carboxylic acid. C4; 10 mM (*black*), 1 mM (*red*), 0.1 mM (*blue*). C6; 10 mM (*black*), 1 mM (*red*), 0.1 mM (*blue*). C8; 2.5 mM (*black*), 0.8 mM (*red*), 0.08 mM (*blue*)

functional groups, Fig. 1) to the isolated ORC under examination. When some of these odorants were put into the perfusion solution, we observed oil films on the surface even after hard shaking and vortex mixing. Because it was important to obtain the practical chemical concentration within the solution, we first measured by GC the amount of odorant molecules in the precise volume of the solution. Also by GC analysis we could check if the chemicals were stable, without reacting to form different substances. In the GC chart, solutions containing the alcohol, ester, or carboxylic acid furnished single peaks, indicating that they caused no chemical reactions (Table 1; Fig. 1). Initially we also examined aldehydes, which are frequently used in flavor and fragrance research. By GC–MS analysis, however, it was confirmed that C4, C6, and C8 aldehydes were partially oxidized, producing carboxylic acids (data not shown), and no further experiments were performed with aldehydes in this work.

When the carbon chain was shorter than C8 (i.e. C4 and C6), the chemicals dissolved perfectly into the solution (up to 10 mM). For C8 substances, however, the maximum concentrations in the solution were lower than 3 mM (Table 1). Because low-concentration solutions (nominal 1 mM, or lower) were prepared by stepwise dilution of solutions of high concentrations (see above), we corrected the concentrations in all data plots to practical values obtained by GC.

When carboxylic acids were dissolved in the perfusion solution, the pH of the solution was shifted to acidic. Because the voltage-gated Na channel is sensitive to pH (see, e.g., Ref. [16]), we adjusted the pH by titration with NaOH. In this study, the titer of NaOH for the carboxylic acid solution was almost identical with that expected for the amount of carboxylic acid measured by GC. This result suggests that carboxylic acids in the perfusion solution were almost completely ionized, irrespective of the length of the carbon chain. In contrast, other chemicals (the alcohol and ester) did not cause pH change.

Transient inward current activated by voltage steps in the isolated ORC

Under the voltage clamp condition of single ORC, application of a depolarizing pulse to −10 mV from the holding

Table 1 Concentration of C8 odorant (mM)

	3 mM	1 mM	0.1 mM	0.01 mM
C8 alcohol	2.7	0.9	0.07	0.007
C8 ester	2.1	0.8	0.08	NA
C8 carboxylic acid	2.5	0.8	0.08	NA

The concentration in the top row is the nominal concentration. Numbers in the table show actual concentrations obtained by GC measurements

voltage (V_h) of −100 mV induced a transient inward current (Fig. 2a). The inward current reached a peak in 2.0 ± 0.6 ms (time to peak, $n = 69$) after the onset of the voltage step. Following the peak, the inward current in turn returned to the zero level immediately; the half decay time was 0.98 ± 0.25 ms ($n = 69$) (Fig. 2a). Thus the voltage-dependent transient inward current had the prerequisite features for the voltage-dependent Na current. In fact, the inward current responses completely disappeared when the external Na^+ was replaced with choline (Fig. 2a). To extract the voltage-gated Na component, the leak component was subtracted from the data (Fig. 2b, c). The peak amplitude of the inward current (I_{Na}) was 229.8 ± 88.1 pA ($n = 69$).

### Electrophysiological properties of voltage-gated Na current

In this section, we further describe the electrical features of the voltage-gated Na current in the newt ORC. In the experiment of Fig. 3a, the depolarizing step was changed from −150 to +90 mV ($V_h = -100$ mV, duration 20 ms). Transient inward currents were observed for depolarizing voltage steps more positive than approximately −60 mV. The I–V relationship had a monotonic U-shape (Fig. 3b). The reversal potential was $+56.5 \pm 3.7$ mV ($n = 5$) with $[Na^+]_i = 11$ mM, $[Na^+]_o = 114.8$ mM. This potential agrees well with the theoretical value of the Nernst potential for Na^+ (+60.0 mV at 24°C). The shape of waveforms, the I–V relationship, and the reversal potential were essentially the same as those obtained in previous work on newt ORCs [17].

The activation curve of I_{Na} was well fitted by the single Boltzmann function

$$RC = \frac{A_1 - A_2}{1 + \exp\left(\frac{V - V_1}{V_2}\right)} + A_2 \qquad (1)$$

where RC is the relative conductance, V the voltage pulse, and A_1, A_2, V_1 and V_2 are the constants obtained by fitting to the data of Fig. 3c, d. The half-activation voltage was -32.5 ± 4.5 mV ($n = 5$) (Fig. 3c), and the half-inactivation voltage was -61.9 ± 1.2 mV ($n = 4$) (Fig. 3d). These values are consistent with those described in previous reports (half activation voltage −34 mV; half inactivation voltage −53 mV [4]).

The transient voltage-gated Na current contained current fluctuations. Because of this, the peak amplitude of the inward current varied among trials, which produced errors in the data analyses (Fig. 3e). To minimize the data error, we averaged the waves recorded 30–100 times with repeatedly applied steps. The possibility that such current fluctuation was caused by the channel gating was verified by observing the variance–mean plot (Fig. 3f) [18].
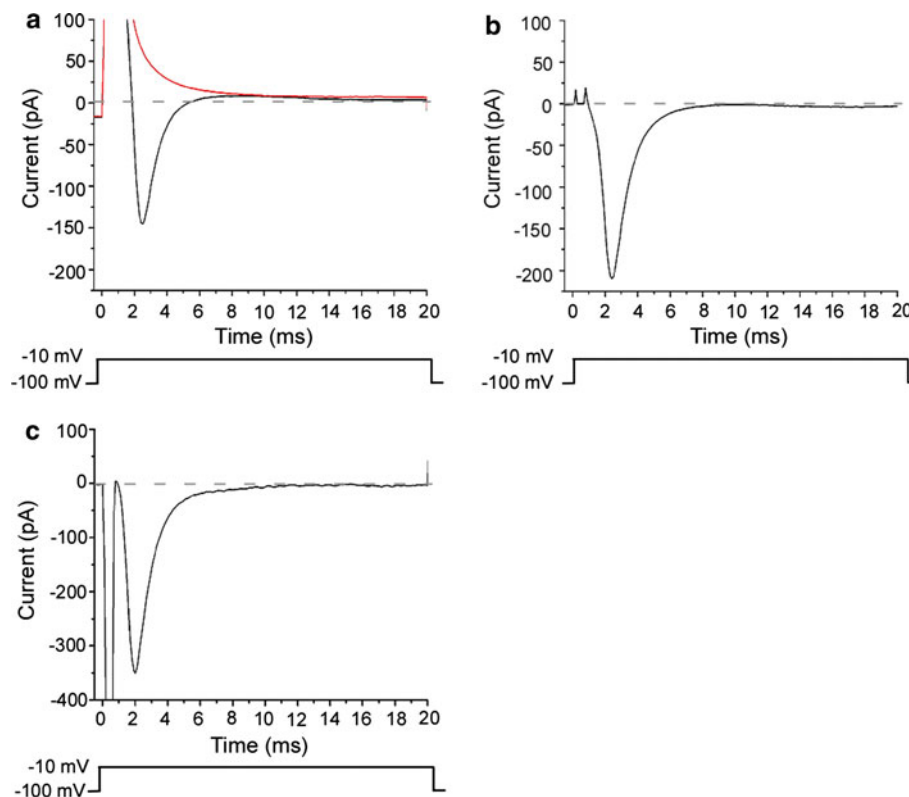
Fig. 2 Voltage-gated Na current. Upward deflection of *bottom trace* indicates the timing and duration of the voltage pulse. **a** Current waveform by depolarization to −10 mV ($V_h = -100$ mV). *Black trace* shows the current in the perfusion solution. *Red trace* shows the current in the choline solution. Averaged waves of the current generated by the 30 times depolarization pulse. **b** Capacitive and leak current subtraction. The current waveforms in **a** were subtracted to show the voltage-gated Na current. **c** The current measured with P/4 subtraction. Membrane current evoked by depolarization to −10 mV ($V_h = -100$ mV). The P/4 subtraction function was supplied with pClamp. Different cell from **a** and **b**. A downward large transient shows a capacitive current. Corrected capacitive current was negative, because the capacitive current in the original trace was over-saturating the range of the A/D converter, whereas the four smaller currents used for subtraction were within the range

$$\sigma^2 = iI - I^2/n \qquad (2)$$

where σ^2 is the variance, I the mean whole-cell current, i the amplitude of single-channel current, and n is the number of channels in the single ORC. The relationship between σ^2 and I could be fitted well by the parabola (Eq. 2), consistent with the idea that the current fluctuation was caused by the channel gatings. The total number of voltage-gated Na channel was 1220 ± 244, and the size of single-channel current was 0.29 ± 0.09 pA ($n = 7$). This value of the single-channel current is slightly smaller than in previous reports for the voltage-gated Na channel of the frog node of ranvier (0.35 pA at $\Delta V = 44$ mV [19]; 0.38 pA, at $\Delta V = 59$ mV [20]), the cultured rat cardiac cell (1.4 pA at $\Delta V = 40$ mV [21]), and the cultured rat muscle cell (1.8 pA at $\Delta V = 100$ mV [18]). There is a possibility that voltage-gated Na channels in the ORC have small unitary events, but this matter was not further analyzed in this work.

Odorant suppression of voltage-gated Na current

It has been shown that the voltage-gated Na current is suppressed by some odorant molecules [4]. The suppression effect seemed to be variable, depending on odorant species. For instance, *n*-amyl acetate suppressed the voltage-gated Na current strongly [5] whereas limonene had little effect (see also Refs. [1, 2]). To understand the functional structure of effective odorants, we examined the effects of 9 odorant molecules that were selected systematically from their structural features that focused on the chain length and functional group. In this work, the suppression ratio (SR, Fig. 4a) was defined by:

$$SR = 1 - \frac{I_o}{I_c} \qquad (3)$$

where SR is the suppression ratio, I_c is the peak amplitude of I_{Na} in the control solution, and I_o is the peak amplitude of I_{Na} in the odorant solution.
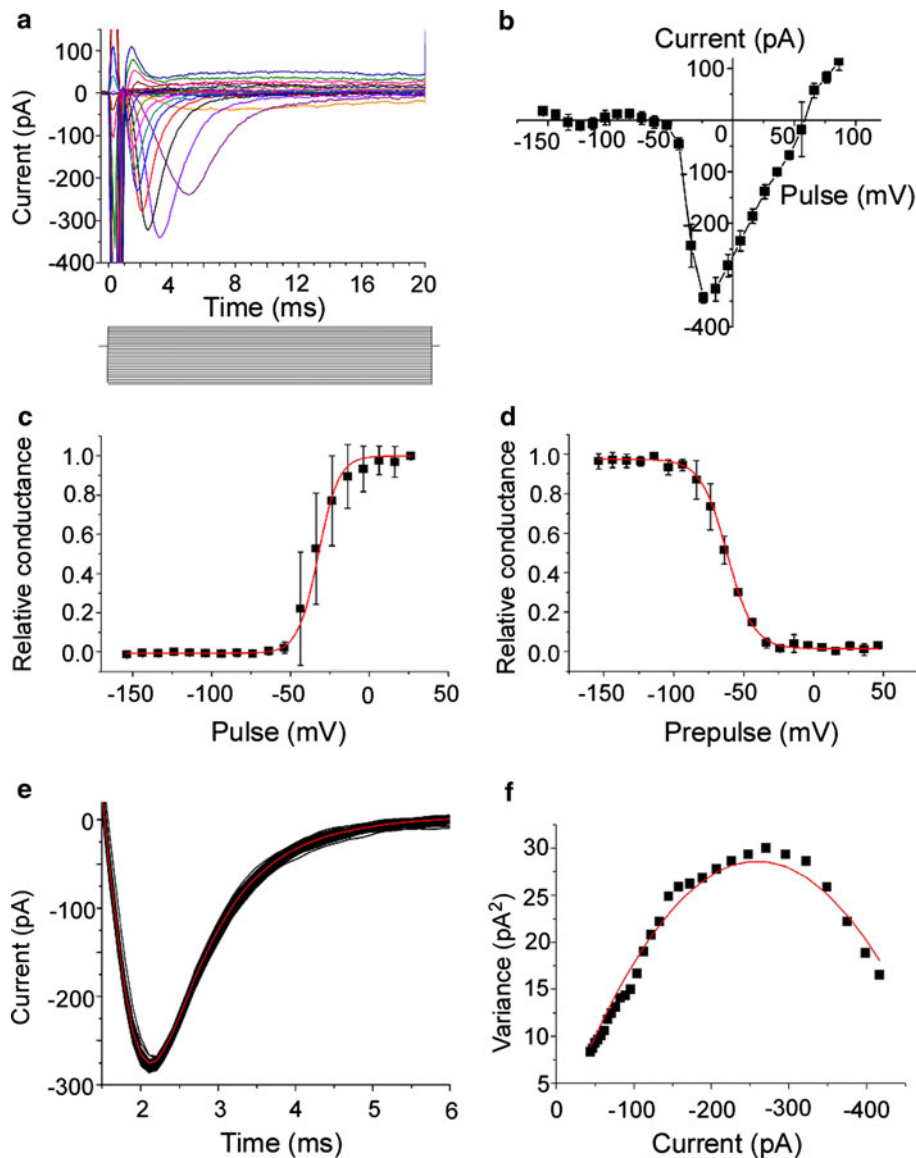
Fig. 3 Electrophysiology of voltage-gated Na channel. Extracellular solution contained 114.8 mM Na. Pipette solution contained Cs. $V_h = -100$ mV. Averaged traces from 3 recordings. Leak currents in **a–d** were subtracted by use of the P/4 function supplied with pClamp. *Error bars* indicate SD. **a** Currents induced by varied voltage steps. Command voltages were increased in 10 mV steps from −150 to +90 mV. The duration of depolarization pulses was 20 ms (*step bar*). **b** I–V relationship for the voltage-gated Na current. Peak currents in **a** were plotted against membrane potentials. Reversal potential was 56.0 mV. **c** Activation curve. The activation curves of I_{Na} were well fitted by the Boltzmann function (see text). Half-activation voltage was −32.5 mV. **d** Inactivation curve. Relative conductances were obtained from the current generated when the −10 mV (100 ms) depolarization pulse was given just after a −150 to 50 mV (1 s) prepulse. The curve was fitted by the same equation as for **c**. Half-inactivation voltage was −61.9 mV. **e** Superimposition of current traces evoked by 100 times depolarization pulse. The depolarization pulse was −10 mV ($V_h = -100$ mV). *Red line* show the average of the currents that was obtained from 100 times recordings. **f** Variance–mean current plot. Data between 2.2 and 5.1 ms in **e** were plotted. *Red trace* is a fit by $\sigma^2 = iI - I^2/n$ (σ^2: variance, i: single-channel current, I: mean current, n: number of channels in a cell), with $n = 2346$, $i = 0.22$ pA. The data were $R^2 = 0.97$ from the least-squares fitting and $\chi^2 = 1.57$ from the chi-squared test

Alcohols reduced the amplitude of voltage-gated Na current in a dose-dependent manner (Fig. 4b). The dose–suppression relationship shifted to the left when the carbon chain number was increased (Fig. 4c). It thus seems likely that the current suppression becomes more obvious with substances having longer carbon chain, which will be further described in the next section by use of the raw data. Suppression was observed with the ester (Fig. 4c; the data will be explained later) but not with the carboxylic acid (Fig. 4c).

Fig. 4 Suppression of voltage-gated Na current by odorants. The voltage-gated Na current was evoked by a depolarization pulse to -10 mV (20 ms) from V_h of -100 mV. The leak current obtained in choline solution was subtracted. **a, b** *Black traces* show currents in control solution, *red trace* currents in odorant solution, *blue trace* current recovery. **a** Reduction of voltage-gated Na current by C6 alcohol (1 mM). Upward deflection of *bottom trace* indicates the timing and duration of the voltage pulse. The suppression ratio is $SR = 1 - \frac{I_o}{I_c}$ (I_c: I_{Na} peak in the control solution, I_o: peak current in the odorant solution). These data show $SR = 0.19$. **b** Suppression of voltage-gated Na current by 3 different concentrations of C6 alcohol. Average of 30 recordings. Upward deflection of *bottom trace* indicates the timing and duration of the voltage pulse. Suppression ratios were -0.51×10^{-2} (0.1 mM), 0.22 (1 mM), and 1.06 (10 mM). **c** Correlation between odorant concentration and suppression ratio. *Black squares* show C8 chemicals (alcohols, esters, and carboxylic acids), *red circles* are C6, and *blue triangles* are C4. *Error bars* show SD. *Numbers in parentheses* indicate the number of trial cells
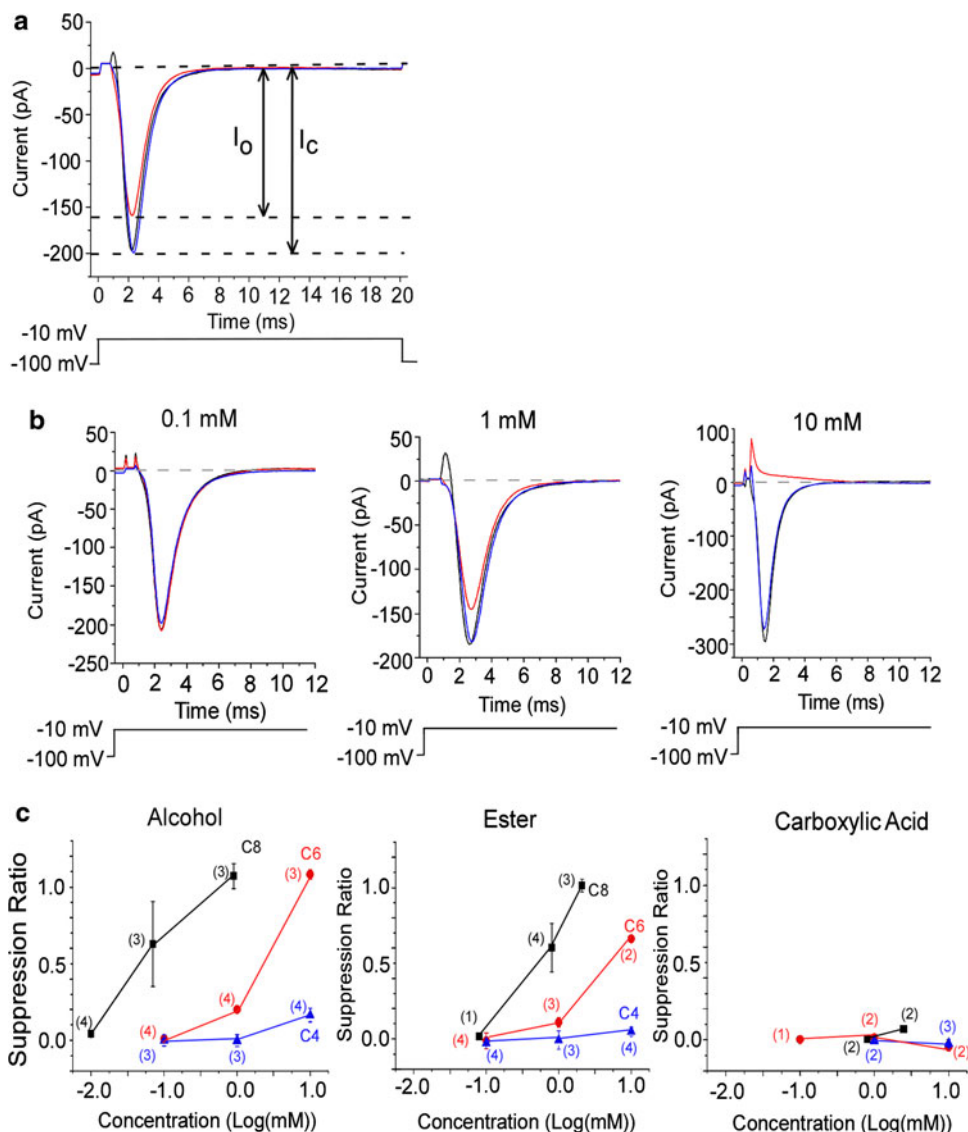
Chain length

Recently, Horishita and Harris [22] showed that the voltage-gated Na channel expressed in Xenopus oocyte membrane is suppressed by *n*-alcohols. They further showed that the suppression becomes more obvious when the number of carbon atoms is increased. This is exactly the same as shown in Fig. 4c in this study. In this section, we focus on the change in the suppression in relation to the length of the main carbon chain for esters and carboxylic acids also.
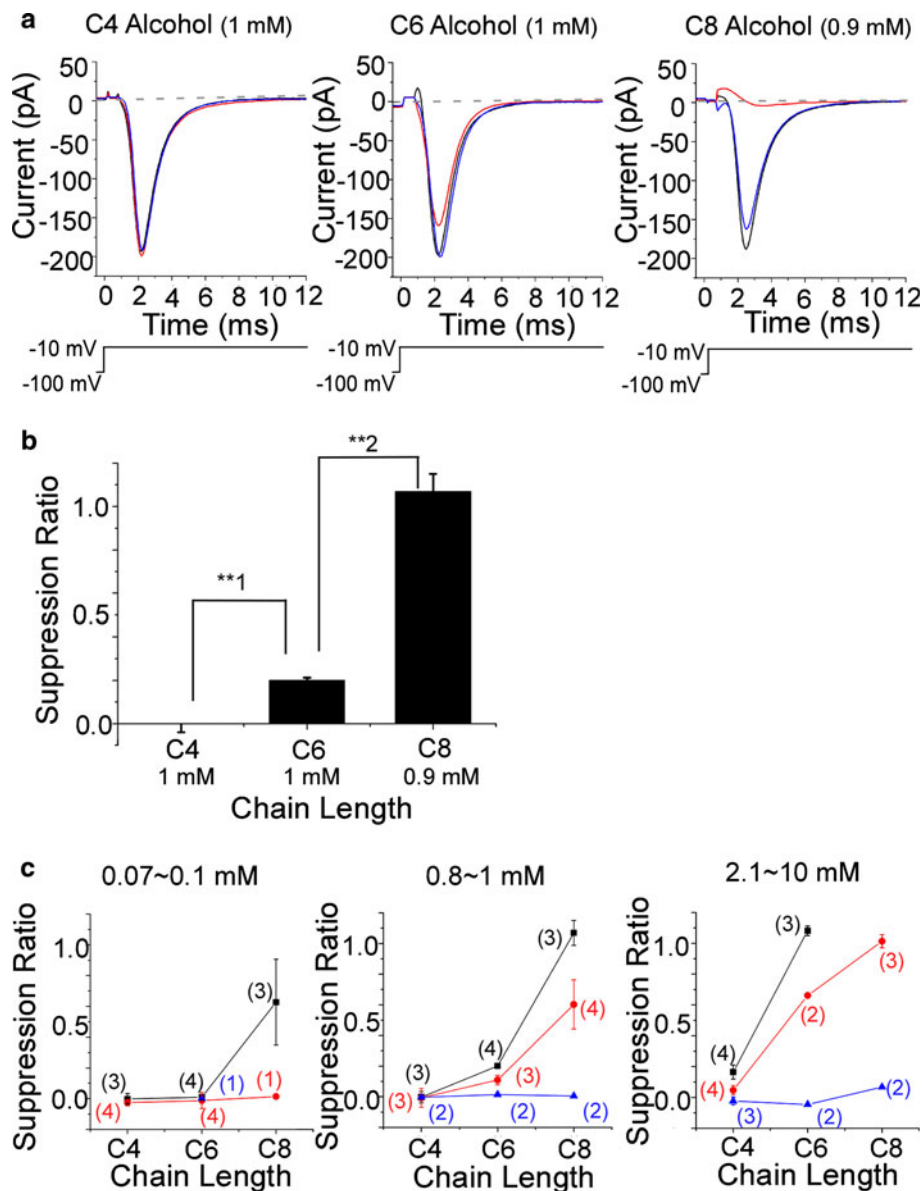
The voltage-gated Na currents were suppressed by C4, C6, and C8 alcohols (Fig. 5a). Suppression ratios increased when the length of the carbon chain was increased (C4–C8) (Fig. 5b). There was statistical significance between C4 alcohol ($n = 4$) and C6 alcohol ($n = 3$) and between C6

alcohol ($n = 4$) and C8 alcohol ($n = 3$) (*t* test, $p < 0.005$). Similar chain dependence was observed for the experiment with the ester (Fig. 5). It is notable that for any length of carbon chain the suppression ratio was larger for the alcohol than for the ester. No remarkable suppression of the voltage-gated Na current was observed for carboxylic acids under all the conditions used in this work (Figs. 4c, 5c, see also later).

These results suggest that the suppression induced by both the alcohol and the ester becomes stronger depending on the length of main chain.

Functional groups

Next, we investigated the relationship between current suppression and functional groups with the same numbers
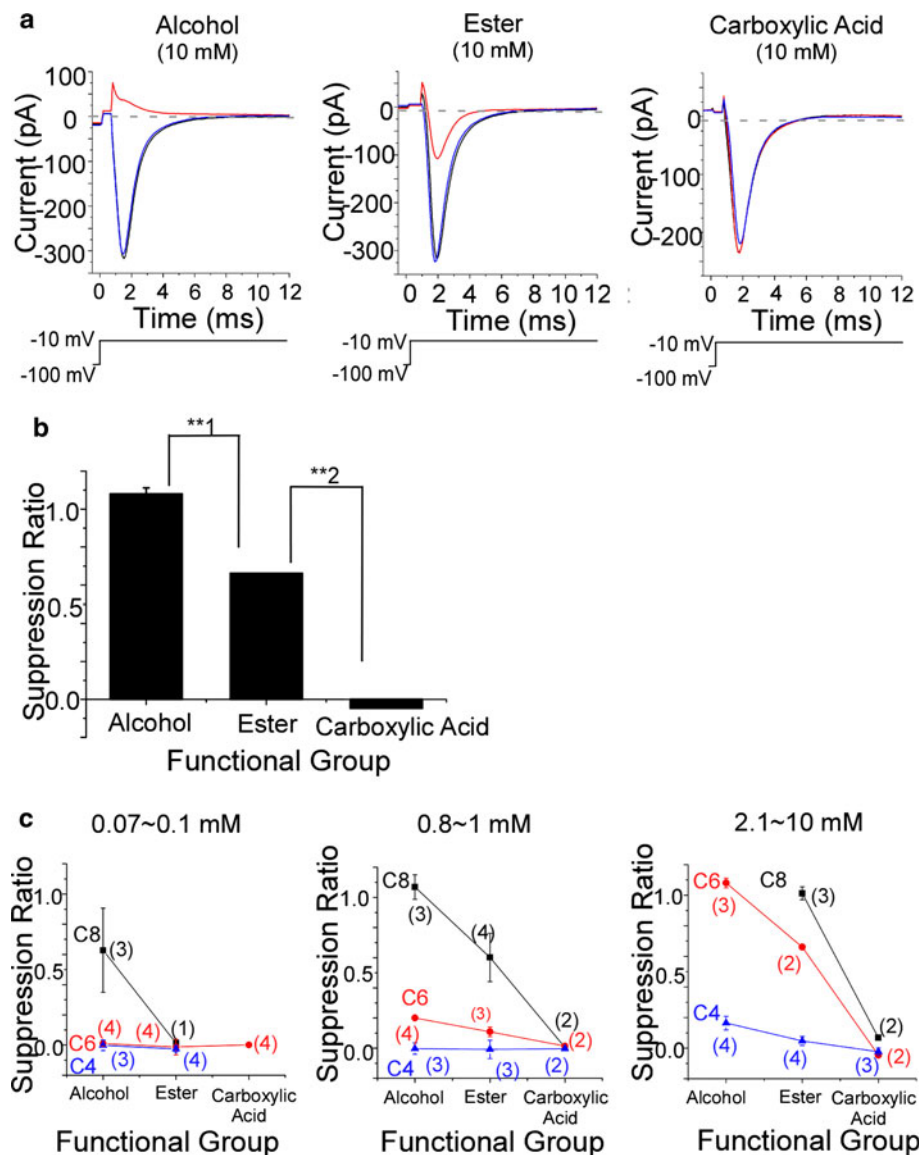
Fig. 5 Dependence of suppression on carbon chain length. The leak current obtained in choline solution was subtracted from all currents. **a** Current waveform in alcohol solution. Alcohol suppressed voltage-gated Na channel current evoked by 20 ms depolarization to -10 mV from V_h of -100 mV. Average from 30 recordings. Upward deflection of *bottom trace* indicates the timing and duration of the voltage pulse. *Black trace* control, *red trace* alcohol, *blue trace* recovery. Suppression ratio for C4 (1 mM) was -0.31×10^{-1}, for C6 (1 mM) was 0.19, and for C8 (0.9 mM) was 0.98. **b** Suppression ratios for alcohols of different carbon chain length. Suppression ratio for C4 (1 mM) was $-0.28 \times 10^{-2} \pm 0.37 \times 10^{-1}$ ($n = 3$), for C6 (1 mM) was $0.20 \pm 0.11 \times 10^{-1}$ ($n = 4$), and for C8 (0.9 mM) was $1.07 \pm 0.81 \times 10^{-1}$ ($n = 3$). Using t test for **1 and **2, $p < 0.005$. **c** Relationship between suppression ratio and carbon chain length.

Left: *black squares* show C8 alcohol (0.07 mM), C6 alcohol (0.1 mM), and C4 alcohol (0.1 mM). *Red circles* show C8 ester (0.08 mM), C6 ester (0.1 mM), and C4 ester (0.1 mM). *Blue triangle*s show C6 carboxylic acid (0.1 mM). *Center*: *black squares* show C8 alcohol (0.9 mM), C6 alcohol (1 mM), and C4 alcohol (1 mM). *Red circles* show C8 ester (0.8 mM), C6 ester (1 mM), and C4 ester (1 mM). *Blue triangles* show C8 carboxylic acid (0.8 mM), C6 carboxylic acid (1 mM), and C4 carboxylic acid (1 mM). *Right*: *black squares* show C6 alcohol (10 mM) and C4 alcohol (10 mM). *Red circles* show C8 ester (2.1 mM), C6 ester (10 mM), and C4 ester (10 mM). *Blue triangles* show C8 carboxylic acid (2.5 mM), C6 carboxylic acid (10 mM), and C4 carboxylic acid (10 mM). *Error bars* show SD. *Numbers in parentheses* indicate the number of trial cells

of carbons. Among three types of C6 chemicals (alcohols, esters, and carboxylic acids), alcohols resulted in the highest suppression ratio. Carboxylic acids resulted in no

current suppression, irrespective of carbon chain length or concentration (Fig. 6c). There were statistical differences between C6 alcohol and C6 ester, and between C6 ester

Fig. 6 Dependence of suppression ratio on functional group. Alcohols, esters, and carboxylic acids were used as odorants in extracellular perfusion solutions. Current was evoked by depolarization to -10 mV (20 ms) from V_h of -100 mV. The leak current obtained in choline solution was subtracted from all current waveforms. **a** Current waveform in solutions of the C6 chemicals. Average of 30 recordings. Upward deflection of *bottom trace* indicates the timing and duration of the voltage pulse. *Black trace* control, *red trace* odorant, *blue trace* recovery. The suppression ratio for the alcohol (10 mM) was 1.11. That for the ester (10 mM) was 0.66. That for the carboxylic acid (10 mM) was -0.50×10^{-2}. **b** Suppression ratio for each functional group. Suppression ratio for C6 alcohol (10 mM) was $1.08 \pm 0.31 \times 10^{-1}$ ($n = 3$), that for C6 ester (10 mM) was 0.66 ($n = 2$), that for C6 carboxylic acid (10 mM) was -0.46×10^{-1} ($n = 2$). Using *t* test for **1 and **2, $p < 0.005$. **c** Relationship

between suppression ratio and carbon chain length. *Left*: *black squares* were C8 alcohol (0.07 mM) and C8 ester (0.08 mM). *Red circles* were C6 alcohol (0.1 mM), C6 ester (0.1 mM), and C6 carboxylic acid (0.1 mM). *Blue triangles* were C4 alcohol (0.1 mM) and C4 ester (0.1 mM). *Center*: *black squares* were C8 alcohol (0.9 mM), C8 ester (0.8 mM), and C8 carboxylic acid (0.8 mM). *Red circles* were C6 alcohol (1 mM), C6 ester (1 mM), and C6 carboxylic acid (1 mM). *Blue triangles* were C4 alcohol (1 mM), C4 ester (1 mM), and C4 carboxylic acid (1 mM). *Right*: *black squares* were C8 ester (2.1 mM) and C8 carboxylic acid (2.5 mM). *Red circles* were C6 alcohol (10 mM), C6 ester (10 mM), and C6 carboxylic acid (10 mM). *Blue triangles* were C4 alcohol (10 mM), C4 ester (10 mM), and C4 carboxylic acid (10 mM). *Error bars* show SD. *Numbers in parentheses* indicate the number of trial cells. Data shown in **c** were obtained from Fig. 5c

and C6 carboxylic acid (*t* test, $p < 0.005$) (Fig. 6b). At any carbon length, this sequence was preserved. It thus seems likely that the alcohol causes stronger suppression than the ester or carboxylic acid.

Suppression of CNG channel in the ORC

In previous sections it has been shown that the voltage-gated Na channel is suppressed by several types of

odorants. The suppression was dominant with the alcohol, and became larger when the chain length was increased. We wondered whether this tendency was also observed for the CNG channel that is directly responsible for olfactory signal transduction.

As has been reported previously [9], application of UV light to olfactory cilia filled with caged cAMP induced an inward current response at -50 mV. Because in this study we omitted Ca^{2+} from the external solution, this inward current represents a nearly pure CNG channel component. When C4, C6, and C8 alcohol were applied to the cilia together with the UV light, the cAMP-induced responses reduced their amplitudes (Fig. 7a–c). The degree of suppression was biggest with C8 alcohol and the SR was reduced when the chain length was shortened (Fig. 7d). When the functional group was changed to the ester, SR was also reduced (Fig. 7e, f). With the C8 carboxylic acid, we did not observe suppression in cAMP-induced responses (Fig. 7g, h). Thus, the CNG channel is also suppressed by these odorants with almost the same tendency as the voltage-gated Na channel.

Relationship between distribution coefficient and suppression of ion channels

In previous sections it has been shown that odorant suppression of ion channels depends on the length of the main chain and the concentration of the chemicals. On the basis of these findings it was thought that solubility and hydrophobicity are, at least in part, responsible for the expression of suppression. But carboxylic acids did not cause any detectable suppression, even with the same length of carbon chain. Initially, these differences were thought to be solely because of the change in the structure of the functional group, not because of general chemical features (see, e.g., hydrophobicity) of the molecules. In fact, the carboxylic acids have almost the same octanol/water partition coefficients (Log P [23]) as the alcohols and esters. Throughout the analyses, however, we noticed that the suppression could be described by Log D (distribution coefficient) that is actually an index of the hydrophobicity of molecules within the organisms. Log D is similar to Log P measured for the octanol/water boundary, except that the former takes pH buffer into account whereas the latter does not.

The relationship between the current suppression (alcohols, esters and carboxylic acids together) and Log D was plotted in Fig. 8a, b. The values of Log D (pH. 7.4) were obtained from ChemSpider provided by the Royal Society of Chemistry (RSC, no data were obtained for C4 and C6 carboxylic acids presumably because they partition almost exclusively into the aqueous phase; substances having shorter carbon chains have smaller

Log D value). In Fig. 7b, the CNG current suppression ratio that obtained by puff application was larger than that obtained for Na current suppression measured by use of the U-tube system. As we have reported previously, the concentrations of drugs that were applied by puff application is reduced by dilution by the surrounding media [3], whereas with the U-tube system the stimulus concentration is almost identical with that of the applied solution. It is possible to assume:

1 that CNG channels are suppressed more efficiently than Na channels; or
2 that the ciliary structure may lead to highly efficient suppression compared with the cell body.

In this study, no further experiments were conducted to resolve these possibilities.

Discussion

In this study, we investigated the effect of odorants on ion channels to understand how the functional structure of odorant molecules affects channel suppression. Suppression became stronger for the alcohols and esters when the chain length was increased. Even with the same length, however, the carboxylic acids, which have small Log D values, did not cause suppression. These results support the notion that the odorant molecules dissolve (and/or bind) to hydrophobic sites within the plasma membrane. It is unlikely that there is a particular binding site within the channel molecule, because the suppression is induced by varieties of odorants having distinct structures [1–4, 24, see also 25] and in different types of ion channels. It is possible to assume that odorants are integrated with the lipid bi-layer, and cause conformational changes universally in ion channels.

Relationship between the length of the main chain and odorant suppression

Horishita and Harris [22] have examined the effect of alcohol on Nav1.2, Nav1.4, Nav1.6, or Nav1.8 expressed in Xenopus oocyte membrane. They showed that the alcohol reduced voltage-gated Na current through Nav1.2, Nav1.4, and Nav1.6, but did not affect Nav1.8. Although the subgroup of the voltage-gated Na channel expressed in the newt ORC used in this study has not yet been identified, it seems unlikely that the channel is solely of the Nav1.8 type. Interestingly, the alcohol suppression of Nav1.2, Nav1.4, and Nav1.6 became stronger when the carbon chain was increased, as similarly shown in our work. In addition, we further confirmed that the ester, which is commonly used as a pleasant perfumery compound, shows suppression with similar chain-length dependence. Franks
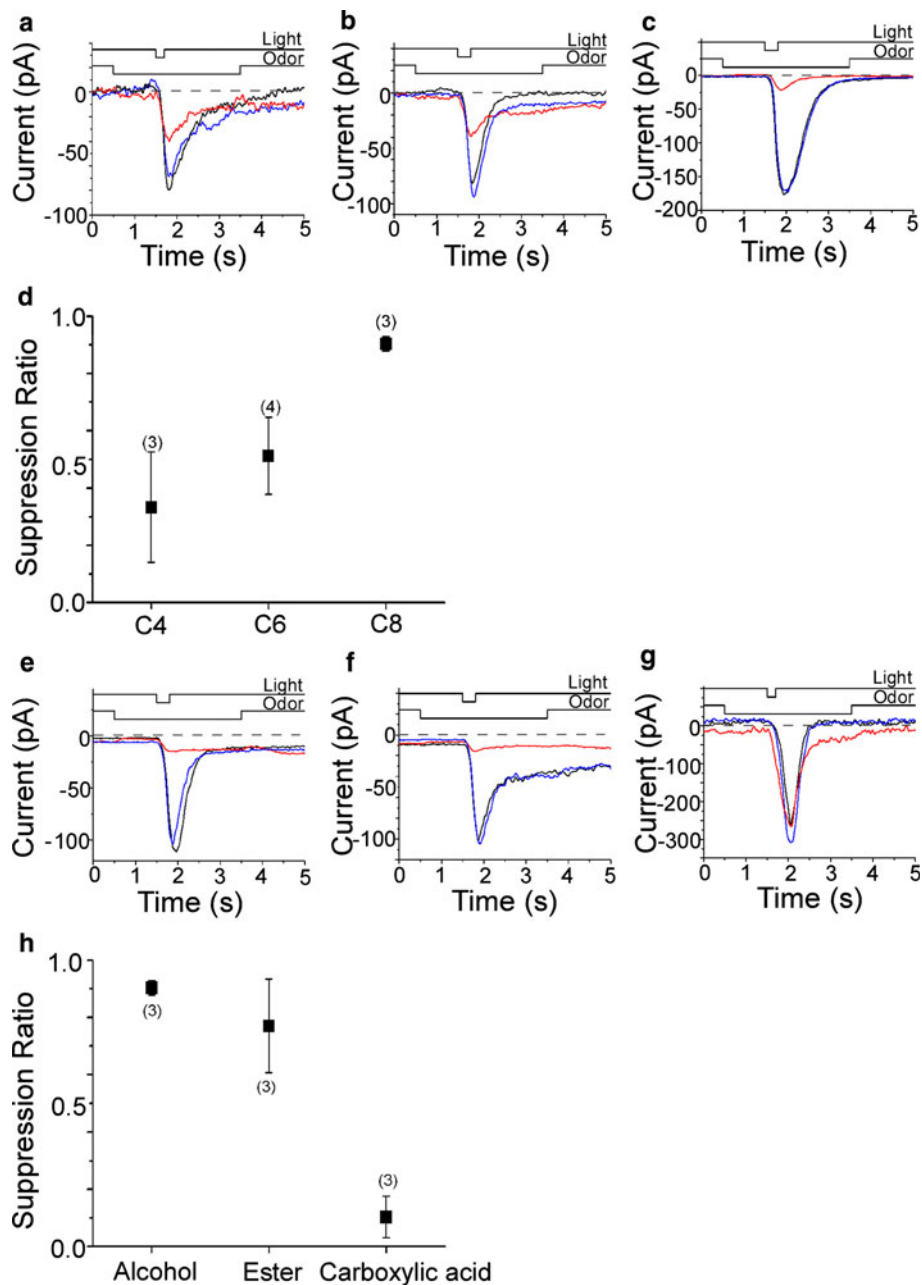
Fig. 7 Suppression of cAMP-induced current by odorants. **a** Effect of 1 mM C4 alcohol on the cAMP-induced current. Odorant concentrations were 1 mM except for C8 alcohol (0.9 mM), C8 ester (0.8 mM), and C8 carboxylic acid (0.8 mM). After the light-induced current was recorded as a control (*black*), odorant was applied before light stimulation to cover the response period observed in the control (*red*). Pressure of odor stimulation was 50 kPa, duration was 3 s. Duration of the light stimulation was 200 ms. After a 20-s interval, the light stimulation was again applied in the absence of chemical (*blue*) to confirm the recovery. Downward deflection of the *upper traces* indicates the timing and duration of the light and odor stimulation. $V_h = -50$ mV. Light stimulation was 0.62, as a relative value in our setup (see Ref. [9]). SR = 0.54. **b** Effect of 1 mM C6 alcohol on the cAMP-induced current. Light stimulation was 0.37. SR = 0.68. **c** Effect of 1 mM C8 alcohol on the cAMP-induced current. Light stimulation was 0.62. SR = 0.88. **d** Relationship between chain length of *n*-alcohols and suppression ratio. **e** Effect of 0.9 mM C8 alcohol on the cAMP-induced current. Light stimulation was 0.62. SR = 0.9. **f** Effect of 0.8 mM C8 ester on the cAMP-induced current. Light stimulation was 0.48. SR = 0.91. **g** Effect of 0.8 mM C8 carboxylic acid on the cAMP-induced current. Light stimulation was 0.62. SR = 0.14. **h** Relationship between functional groups and suppression ratio. *Error bars* show SD. *Numbers in parentheses* indicate the number of cells

and Lieb [26] have also shown that the NMDA receptor channel is suppressed by the alcohol. Again, the suppression became stronger when the carbon chain was increased.

They proposed that hydrophobicity was an important factor for the alcohol suppression of the NMDA receptor channel.
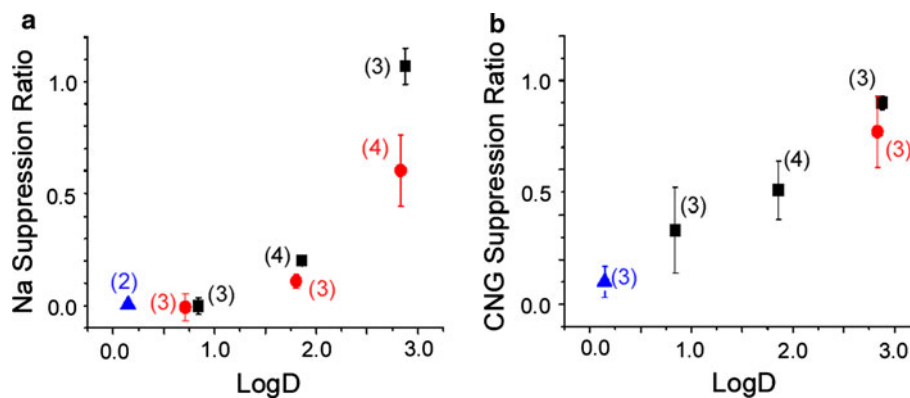
Fig. 8 Relationship between hydrophobicity and suppression ratio. Odorant concentrations were 1 mM except for C8 alcohol (0.9 mM), C8 ester (0.8 mM), and C8 carboxylic acid (0.8 mM). *Black squares* alcohol, *red circles* ester, *blue triangles* carboxylic acid. *Error bars* show SD. *Numbers in parentheses* indicate the number of cells.

a Relationship between octanol/water distribution coefficient (Log D) and suppression ratio of the Na current. The longer the chain, the larger the value of Log D. There were no Log D data for C4 and C6 carboxylic acids. **b** Relationship between Log D and suppression ratio of the cAMP induced current

Furthermore, alcohols suppress ATP-dependent channels in the dorsal ganglion cells of the bull frog only when the chain length is shorter than four [27]. In this preparation, the suppression became stronger when the chain length was reduced. They supposed there was a binding pocket for the small alcohol molecule within the ATP-dependent channel.

As for blockage of ion channels by amphiphilic drugs, Lundbaek [28] proposes that the lipid bi-layer of the plasma membrane is modulated structurally by amphiphile molecules. On the basis of cumulative observations, Andersen et al. [29] concluded that the conformational changes of ion channels are accompanied by physico-chemical changes of the surrounding lipid bi-layer. It is worth investigating whether carboxylic acids, which did not cause suppression in this work, change the physico-chemical structure of the lipid bi-layer.

The olfactory signal transduction channel, the CNG channel, has been also shown to be suppressed by odorants [2]. Observed odorant suppression was strong when the channel was assembled with CNGA2, CNGA4, and CNGB1 (the native form of the CNG channel [30]) whereas odorant suppression was not observed for the homo-oligomer channel made of the principle subunit (CNGA2). There may be effective sites in both (either) CNGA4 and (or) CNGB1, or, the channel function is more drastically affected in the hetero-oligomer channel by an odorant-induced change of the bi-layer mechanical energy.

In this study, odorant suppression of the channel by both the alcohol and ester was shown to be variable depending on the length of the carbon chain (from C4 to C8). Furthermore, there was a relationship between suppression and Log D of the chemicals. These observations are consistent with the idea that the odorant dissolves in (and/or binds to) hydrophobic sites within the plasma membrane.

Relationship between functional group and suppression of the voltage-gated Na channel

The alcohol has a slightly larger effect than the ester on channel suppression. This may be because the alcohol has slightly a higher Log D value than the ester. It is also interesting to note that the length of the continuous carbon chain is longer in the alcohol than in the ester when the total number of carbon is the same. In fact in Fig. 4, the position of the dose-suppression curve for the C8 ester is between those for the C6 alcohol and the C8 alcohol. These results also support the notion that hydrophobicity is a key factor determining odorant suppression of ion channels.

In contrast, carboxylic acids did not cause detectable changes in the voltage-gated Na channel, even with the C8 compound and with 10 mM concentration. The most remarkable difference of carboxylic acids from other compounds used here is the tendency for ionization. Because of this, carboxylic acids partition almost exclusively into the aqueous phase, with extremely low Log D values. Although we did not examine longer-chain compounds, Xiao et al. [31] have reported that carboxylic acids with longer chains (C15–C22) have the ability to suppress $Na_V1.5$ channels expressed in HEK 293 cells. Because of the long chain, these compounds would have high hydrophobicities. These observations are all consistent with the notion that channel suppression is correlated with the hydrophobicity of the compound.

Channel suppression in the ORC and olfactory masking

This study shows that voltage-gated Na channels in the ORC are suppressed by variety of odorants (see also Ref. [4]). At this moment, we do not know if such suppression occurs in vivo. Voltage-gated Na channels are distributed

in the dendro-somatic membrane whereas under natural conditions the odorant molecules are delivered to the mucus. At the same time, volatile substances are very hydrophobic, as has been shown also in this work, and, therefore, membrane permeable. There is a possibility that the odorant can pass through the membrane structure to gain access to voltage-gated Na channels. To reach a conclusion, we have to measure the absolute concentration of odorant molecules in the interstitial area when the natural stimulants are applied to the surface of the epithelium; this has not yet been performed. Nevertheless, we have to pay attention to the experiments and interpretation of spiking responses when we use solitary cells or slice preparations for research on the odorant effect.

In parallel, in this work, we showed that CNG channels are suppressed by odorants. Odorant suppression of CNG channels was largest with alcohols, compared with esters and carboxylic acids. Furthermore, the suppression became more obvious when the chain length was increased. These properties matched exactly to those observed in the voltage-gated Na channel. The results suggest that the blockage by odorants of both CNG and Na channels share the same step(s).

Odorant suppression of the CNG channels had similar odor-dependence to human masking [3]. Furthermore, it has been shown that odorant molecules that have been absorbed from the air have ability to suppress CNG channels beyond the air/water boundary, indicating that the suppression occurs in the nose. It thus seems highly likely that olfactory masking is, at least in part, regulated by the blockage of CNG channel by odorants. It is therefore highly likely that these chemicals represent the molecular structures inducing olfactory masking, and that the results obtained here will provide information about the development of novel masking agents based on the molecular architecture. Na channels may provide powerful tools for rapid and convenient screening.

References

1. Kurahashi T, Lowe G, Gold HG (1994) Suppression of odorant responses by odorants in olfactory receptor cells. Science 265:118–120
2. Chen TY, Takeuchi H, Kurahashi T (2006) Odorant inhibition of the olfactory cyclic nucleotide-gated channel with a native molecular assembly. J Gen Physiol 128:365–371
3. Takeuchi H, Ishida H, Hikichi S, Kurahashi T (2009) Mechanism of olfactory masking in the sensory cilia. J Gen Physiol 133:583–601
4. Kawai F, Kurahashi T, Kaneko A (1997) Nonselective suppression of voltage-gated currents by odorants in the newt olfactory receptor cells. J Gen Physiol 109:365–372
5. Kawai F, Kurahashi T, Kaneko A (1997) Quantitative analysis of Na^+ and Ca^{2+} current contributions on spike initiation in the newt olfactory receptor cell. Jpn J Physiol 47:367–376
6. Kurahashi T (1989) Activation by odorants of cation–selective conductance in the olfactory receptor cell isolated from the newt. J Physiol 419:177–192
7. Hamill OP, Marty A, Neher E, Sakmann B, Sigworth JF (1981) Improved patch-clamp techniques for high-resolution current recording from cells and cell-free membrane patches. Pflügers Arch 391:85–100
8. Ito Y, Kurahashi T, Kaneko A (1995) Pressure control instrumentation for drug stimulation. Nippon Seirigaku Zasshi 57:127–133
9. Takeuchi H, Kurahashi T (2002) Photolysis of caged cyclic AMP in the ciliary cytoplasm of the newt olfactory receptor cell. J Physiol 541:825–833
10. Hille B (1967) The selective inhibition of delayed potassium currents in nerve by tetraethylammonium ion. J Gen Physiol 50:1287–1302
11. Trotier D (1986) A patch-clamp analysis of membrane currents in salamander olfactory receptor cells. Pflügers Arch Eur J Physiol 407:589–595
12. Rajendra S, Lynch WJ, Barry HP (1992) An analysis of Na^+ currents in rat olfactory receptor neurons. Pflügers Arch Eur J Physiol 420:342–346
13. Suzuki S, Tachibana M, Kaneko A (1990) Effects of glycine and GABA on isolated bipolar cells of the mouse retina. J Physiol 421:645–662
14. Fenwick EM, Marty A, Neher E (1982) A patch-clamp study of bovine chromaffin cells and of their sensitivity to acetylcholine. J Physiol 331:577–597
15. Krishtal OA, Pidoplichko IV (1980) A receptor for protons in the nerve cell membrane. Neuroscience 5:2325–2327
16. Hille B (1968) Charges and potentials at the nerve surface. Divalent ions and pH. J Gen Physiol 51:221–236
17. Narusuye K, Kawai F, Matsuzaki K, Miyachi E (2005) Linalool suppresses voltage-gated currents in sensory neurons and cerebellar Purkinje cells. J Neural Transm 112:193–203
18. Sigworth FJ, Neher E (1980) Single Na^+ channel currents observed in cultured rat muscle cells. Nature 287:447–449
19. Conti F, Hille B, Neumcke B, Nonner W, Stämpfli R (1976) Measurement of the conductance of the sodium channel from current fluctuations at the node of Ranvier. J Physiol 262:699–727
20. Sigworth FJ (1980) The variance of sodium current fluctuations at the node of Ranvier. J Physiol 307:97–129
21. Cachelin AB, De Peyer EJ, Kokubun S, Reuter H (1983) Sodium channels in cultured cardiac cells. J Physiol 340:389–401
22. Horishita T, Harris AR (2008) n-Alcohols inhibit voltage-gated Na^+ channels expressed in Xenopus oocytes. J Pharmacol Exp Ther 326:270–277
23. Philip HH, William MM (1997) Handbook of physical properties of organic chemicals. Syracuse Research Corporation, Syracuse
24. Yamada H, Nakatani K (2001) Odorant-induced hyperpolarization and suppression of cAMP-activated current in newt olfactory receptor neurons. Chem Senses 26:25–34
25. Reisert J (2010) Origin of basal activity in mammalian olfactory receptor neurons. J Gen Physiol 136:529–540
26. Franks NP, Lieb RW (1986) Partitioning of long-chain alcohols into lipid bilayers: Implications for mechanisms of general anesthesia. Proc Natl Acad Sci USA 83:5116–5120
27. Li C, Peoples WR, Weight FF (1994) Alcohol action on a neuronal membrane receptor: evidence for a direct interaction with the receptor protein. Proc Natl Acad Sci USA 91:8200–8204
28. Lundbaek JA (2008) Lipid bilayer-mediated regulation of ion channel function by amphiphilic drugs. J Gen Physiol 131:421–429

29. Andersen OS, Nielsen C, Maer MA, Lundbaek AJ, Goulian M, Koeppe ER (2010) Ion channels as tools to monitor lipid bilayer–membrane protein interactions: gramicidin channels as molecular force transducers. In: Essential ion channel methods. Academic Press, Burlington, pp 315–333

30. Shapiro MS, Zagotta NW (1998) Stoichiometry and arrangement of heteromeric olfactory cyclic nucleotide-gated ion channels. Proc Natl Acad Sci USA 95:14546–14551

31. Xiao YF, Wright NS, Wang KG, Morgan PJ, Leaf A (1998) Fatty acids suppress voltage-gated Na^+ currents in HEK293t cells transfected with the alpha-subunit of the human cardiac Na^+ channel. Proc Natl Acad Sci USA 95:2680–2685